

<https://doi.org/10.30678/fjt.162698>

© 2025 The Authors

Open access (CC BY 4.0)

## ENHANCING PROCESSING CAPACITY OF PRECISION PARTS VIA VACUUM LASER DIFFUSION BORON-CHROMIZING

Alakbar Huseynov<sup>1</sup>, Farid Huseynli<sup>2,\*</sup><sup>1</sup>Azerbaijan Technical University, Baku, Azerbaijan; [h\\_alakbar@aztu.edu.az](mailto:h_alakbar@aztu.edu.az); ORCID 0009-0005-5299-1103<sup>2</sup>Azerbaijan Technical University, Baku, Azerbaijan; ORCID 0009-0007-5393-9440\*Corresponding author: [farid.huseynli@aztu.edu.az](mailto:farid.huseynli@aztu.edu.az), +994509614725

### ABSTRACT

The study investigates the improvement of surface strength and reliability of fuel pump precision parts by forming wear-resistant boron–chromium diffusion layers using vacuum laser diffusion boron-chromizing with paste application. Plungers made of steels XBI, IIIX15 and P18 were coated with boron–chromium paste and treated by vacuum laser diffusion metallization. The diffusion layer thickness and microhardness were measured using a PMT-3 tester, while the phase composition and microstructure were analysed by X-ray diffraction and metallography. The process produced boride-rich diffusion layers with thicknesses of about 0.17–0.35 mm and surface microhardness in the range of 18–21 GPa. The maximum microhardness reached 21.0 GPa for XBI, 18.6 GPa for IIIX15 and 17.6 GPa for P18, with minimum values in the diffusion zone remaining above 8.8–11 GPa. X-ray analysis confirmed that complex iron–chromium borides with dominant low-boride (Fe,Cr)<sub>2</sub>B phases are formed. A fine network of surface microcracks acts as a stress-relief mechanism, redistributing residual stresses in the coating. These results show that vacuum laser diffusion boron-chromizing with paste application is a promising technology for restoring and strengthening fuel pump precision parts and creates a solid basis for subsequent tribological testing under service-like conditions.

**Keywords:** boron-chromizing, laser surface hardening, diffusion coating, microhardness, residual stress

### 1. Introduction

One of the key challenges in modern machine building is to improve the reliability and service life of precision parts operating under severe contact and cyclic loads, such as the plunger–barrel pairs in high-pressure fuel pumps. During long-term operation these parts are subjected to high contact stresses, pressure fluctuations and boundary lubrication, which lead to intensive wear, loss of tightness and a decrease in overall pump efficiency.

Conventional surface-hardening and restoration methods – such as induction hardening, carburizing, nitriding, hard chromium plating and thermal spraying – are widely used to increase wear resistance. However, these technologies often fail to provide, simultaneously, high surface hardness, a sufficiently thick hardened layer, strong metallurgical bonding to the substrate and a beneficial compressive residual stress state. In practice they may introduce tensile residual stresses, lead to coating delamination, cause distortion of slender precision parts, or require long high-temperature cycles that are not compatible with tight dimensional tolerances. Classical furnace boriding and boron-based diffusion coatings also improve wear resistance, but their high processing temperatures and long soaking times limit their

applicability to fuel pump precision parts.

Laser-based surface treatments and nanodiffusion coatings formed by paste application offer important advantages over conventional techniques. Localized laser heating in a thin surface layer allows one to create hard diffusion coatings with minimal distortion of the bulk material and to control the thickness and morphology of the modified zone. In particular, complex boron–chromium diffusion layers with a thickness of up to about 0.3 mm occupy a special place among wear-resistant coatings for precision parts because they can combine high hardness with improved corrosion and fatigue behaviour.

At the same time, nanodiffusion coatings produced by laser paste deposition may develop significant internal residual stresses due to differences in crystal lattice parameters and thermal expansion coefficients between the coating and the base metal. Under variable or high constant loads such coatings can crack or delaminate, and in some cases the coated component may fail earlier than an uncoated one. In vacuum diffusion coatings obtained by laser paste deposition, failure is often associated with brittleness of the surface layer or insufficient diffusion bonding with the substrate. Thus, the stress state in the coating, the formation and role of microcracks, and the

interaction between coating and substrate are critical for operational reliability but are not yet fully understood.

Most previous studies on laser surface hardening and boron-based diffusion coatings have focused either on microhardness and phase composition or on wear behaviour of relatively simple geometries. Systematic investigations of vacuum laser diffusion boron-chromizing with paste application on real fuel pump precision parts made of steels XBF, IIIX15 and P18, including the coupled analysis of microstructure, microhardness depth profiles and residual stress distribution in the diffusion layer, remain limited. In particular, the way in which a controlled network of microcracks can redistribute residual stresses and influence the overall stress state of the surface layer has not been sufficiently quantified.

**Research objects and materials.** The investigations were carried out on fuel pumps of the Unified Fuel Pump and Diesel Pump type. The precision pairs (plungers and barrels) are made from alloyed steels such as XBF (chromium-tungsten-manganese steel), IIIX15 (high-carbon chromium bearing steel) and P18 (high-speed tool steel), which are widely used in the manufacture of fuel pump precision parts.

One of the solutions to the problem of improving the reliability and quality of manufactured products is to use the nanodiffusion technological method in vacuum by applying paste to worn parts during the improvement of the operational characteristics of precision parts and increasing and restoring their surface strength with a laser [1-3]. Nanodiffusion coatings are used by applying paste with a laser to increase the reliability of precision parts of machines and devices. In increasing the surface strength with a laser, wear-resistant coatings of complex boron-chromizing with a thickness of up to 0.3 mm occupy a special place.

Nanodiffusion coatings obtained by laser paste deposition improve some properties of precision parts, but often worsen other, sometimes more important properties of the parts. Internal stresses arise in such nanodiffusion coatings. Diffusion coatings exposed to variable or high constant loads during operation can delamination from the surface of precision parts and become unusable, while uncoated parts may not fail under the same load, but reduce the reliability of the products as a result of corrosion. In vacuum diffusion coatings obtained by laser paste deposition, the breakdown of parts is often due to their brittleness or lack of strong diffusion with the base material.

The most important technological method for improving the wear resistance, fatigue resistance and durability of precision parts is laser surface hardening by applying diffusion coatings [4-5]. Depending on the type of paste and the powder deposited on the surface of the material and the test conditions, the durability of the parts increases by 5-70% [6].

Depending on the intensity and duration of laser radiation, the process may be limited to surface heating and phase transformation or may reach melting; in this

work the regimes correspond to controlled heating without deep melting.

In general, various types of lasers and processing atmospheres are used; in the present study, laser diffusion metallization is carried out in a controlled vacuum nanodiffusion environment [7].

Laser surface processing enables controlled modification of a thin surface layer (typically 0.05–5 mm) with minimal influence on the bulk material, which is attractive for precision parts of fuel pumps and other critical components.

**Purpose of the work.** The aim of the present work is to study the stress distribution and microhardness in the process of increasing and restoring surface strength of fuel pump precision parts by complex boron-chromizing with laser paste deposition under vacuum conditions, and to determine the influence of boron and chromium content in the paste on the properties of the diffusion coating. Special attention is paid to the role of crack formation in vacuum nanodiffusion coatings and its effect on the combined stress state in the coating-substrate system.

**Subject of research:** The study examines the influence of the coating technological process on the linear dimensions, mechanical properties, structure and phase composition of precision parts coated with paste, depending on the parameters of laser vacuum diffusion metallization. By using discrete laser tracks, it is possible to form surface zones with specific shapes, sizes and properties that ensure the required strength, wear resistance and reliability under frictional loading.

**Research objects and materials:** The Unified Fuel Pump and Diesel Pump type fuel pumps are composed of pairs made from alloyed steels such as XBF (Chromium-Tungsten-Manganese), IIIX15 (high-carbon chromium steel), and P18 (High-Speed Steel).

## 2. Research

### 2.1. Materials and methods

**Samples and base materials.** The investigations were carried out on precision plungers of Unified Fuel Pump and Diesel Pump type fuel pumps. The working pairs (plungers and barrels) are made from alloyed steels XBF, IIIX15 and P18, which are widely used for fuel pump precision parts. Before coating, the working surfaces of the plungers were ground and polished to a surface roughness of approximately  $Ra \approx 0.2-0.4 \mu\text{m}$  in order to ensure stable adhesion of the diffusion layer.

The boron-chromium diffusion paste was prepared by mixing a boron-containing powder, a chromium-containing powder and an inorganic binder. The solid phase of the paste contained approximately 36 wt.% boron and 64 wt.% chromium; these powders were dispersed in an inorganic binder with auxiliary additives. The powders were homogenised in a mixer for 12 min to obtain a uniform suspension. The paste was applied to the plunger surface by brushing / dipping to a thickness of about 150  $\mu\text{m}$ , followed by drying at 120 °C for 30 min to remove

volatile components and ensure good adhesion before laser processing.

Laser diffusion metallization was performed in a vacuum chamber evacuated to a residual pressure of  $5 \times 10^{-3}$  Pa. The pressure was monitored by an ionisation gauge and kept approximately constant during processing. The use of a vacuum nanodiffusion environment made it possible to minimise oxidation of the surface and to stabilise the diffusion of boron and chromium into the base metal.

A continuous-wave CO<sub>2</sub> laser with a wavelength of 10.6  $\mu\text{m}$  and a maximum output power of 1000 W was used. The laser beam was focused to a spot diameter of 2.0 mm on the plunger surface. The samples were translated under the beam at a scanning speed of 5 mm/s, with a track overlap of approximately 40 % between adjacent passes. For the regimes used in this study, the nominal laser power during processing was 500 W, which corresponds to a power density of approximately  $1.6 \times 10^4$  W/cm<sup>2</sup> on the treated surface. Each surface region was exposed for an effective heating time of about 1 s per cycle, in accordance with the diffusion treatment conditions ( $T = 1150$  °C;  $\tau = 1$  s; cyclic duration 5–6 min) used in the microhardness analysis.

The surface temperature during laser processing was monitored indirectly using preliminary calibration curves obtained from contact thermocouple and pyrometric measurements, which relate the laser parameters and exposure time to the temperature of the diffusion layer. The regimes were selected so that the maximum surface temperature remained within the interval 1100–1150 °C, sufficient to activate diffusion of boron and chromium without excessive melting or distortion of the precision parts. Between cycles, the parts were allowed to cool in vacuum to avoid thermal shock and large temperature gradients.

The thickness of the diffusion layer and the linear dimensional changes of the coated parts were measured using optical microscopy and micrometric control. The microhardness profiles were determined with a PMT-3 microhardness tester at a constant load, starting from the coating surface and moving towards the substrate with a step of 50  $\mu\text{m}$ . X-ray diffraction was used both for phase analysis of the coatings and for evaluation of the residual stress state in the surface layer. The microstructure was examined on etched cross-sections using an optical microscope at magnifications up to  $\times 450$ .

## 2.2. Stress analysis and crack formation

After the application of a nanodiffusion coating by laser paste application, the surface strength, impact strength, and fatigue resistance increase. Therefore, the concept of "reliability" should be used in cases where nanodiffusion coatings increase the operational properties (wear and corrosion resistance, durability, etc.). Depending on the material deposited in nanodiffusion coating, different layer thicknesses and microhardness are achieved in the surface layer [8]. Laser paste vacuum nanodiffusion coatings are

highly resistant to wear and corrosion. The difference in the parameters of the crystal lattices of the nanodiffusion coating and the base metal, as well as their volumetric expansion coefficients, leads to the formation of residual stresses, which in some cases leads to cracking and delamination of the coating.

Laboratory tests are carried out to determine the fatigue resistance of coated parts at a frequency of 2000–6000 rpm based on (5–20)  $\cdot 10^6$  cycles. Based on the results of such tests, predictions are made for all types of parts, which can lead to a decrease in performance, since in most cases the parts are operated under conditions completely different from the test conditions. For example, a relatively small number of repeated loadings of the moving scale can lead to a sharp decrease in the service life of precision parts such as plungers and barrels and other structures (low cycle life). The time factor plays a very important role here.

When an external load is applied, cracks may form and local stresses may arise that are several times higher than the stresses present in the part far from the cracks. The increase in stress at the bottom of various types of scratches, cuts, holes, and transition surfaces, which is a result of design, technological, and operational factors during elastic deformation, is called the stress concentration coefficient.

$$\alpha_K = \frac{\sigma_{\max}}{\sigma_n}$$

where  $\sigma_{\max}$  - the largest axial stress;  $\sigma_n$  - is the nominal stress.

The depth of cracks can be either deep or shallow, depending on the ratio of the crack depth to the component's dimensions. When the surface of worn components is hardened and restored by laser treatment, fewer cracks may occur in regions with lower stress concentrations, such as cracks in the coating and risks after mechanical processing. The concentration of stress depends on the size, number, and relative positioning of the cracks [9, 10]. At this stress level, the effect of cracks is several times stronger than the upper stresses of the coating. This is explained by the fact that as stress increases at the bottom of one crack, the stress at other cracks decreases, which in turn leads to a reduction in the surface stress. This behavior of cracks contributes to a more uniform distribution of stresses and less impact on the strength characteristics of the components, which highlights the positive role of cracks formed inside due to stress. However, an increase in the number of cracks and their proximity to each other may amplify the stress concentration. Alloyed steels are less sensitive to stress concentration compared to brittle metals. Since precision parts of modern machinery and equipment are made from alloyed steels, the formation of cracks in the coating does not have a significant impact. Cracks in coatings, however, may lead to the creation of high stress concentrations due to their growth and deepening [11].

Residual stresses arise due to changes in the volume of the nanodiffusion coating. After the cracks are formed,

each area of the coating bounded by the cracks will continue to tend to compress, thereby deepening the existing cracks. If compressive stresses are formed in the surface layer of the steel, the total stresses in the coating and the steel sample will be distributed as shown in Figure 1. Figure 1 illustrates the evolution and redistribution of stresses in the boron-chromium diffusion layer and the XBF base steel before and after laser nanodiffusion boron-chromizing. In Figure 1a, prior to the formation of the boron-chromium coating, curves 1-4 represent the individual contributions of compressive stresses introduced by mechanical finishing (curve 1), stresses remaining after thermal treatment (curve 2), stresses generated during cyclic diffusion normalisation (curve 3), and temperature-induced stresses (curve 4). Their superposition gives the total stress distribution in the surface layer, shown by curve 5. In Figure 1b, after laser diffusion boron-chromizing and the formation of a surface crack in the coating, the local tensile stresses at the crack tip increase, whereas the stresses in the surrounding regions are partially relaxed. As a result, the overall stress field in the coating-substrate system is redistributed: the crack acts as a stress-relief feature that reduces the effective stress level away from the crack tip, while concentrating tensile stresses in a narrow zone at the crack root.

In this case, before the cracks appear in the coating layer, the total stresses in the surface layer of the steel will be compressed. After the crack is formed in the nanodiffusion coating, due to the concentration of stress, the stresses arising from the coating and the applied layer will increase sharply, and the total stresses in the surface layer of the steel sample will be subjected to tensile force. If the surface layer of the steel sample has tensile stresses before bending, there will be an even stronger total tensile stress. The number of cracks (porosity) on the surface of the coating will depend on the laser processing modes and the deposited material and will improve in terms of quality [12, 13].

### 3. Discussion

One of the most important properties of vacuum nanodiffusion coatings applied using laser-assisted paste deposition to enhance the wear resistance of parts is their hardness. The coating thickness meets technical requirements while allowing for subsequent mechanical processing. The microhardness is measured using a PIMT-3 device and ranges between 18–20 GPa.

Statistical analysis of microhardness data was carried out in order to assess the scatter of the measurements. At each distance from the coating surface at least five indentations were made under identical loading conditions. For every depth, the mean microhardness value and the corresponding standard deviation were calculated and used to construct the profiles shown in Figure 3. The relatively small standard deviations obtained for steels XBF, IIIX15 and P18 confirm the good repeatability of the measurements and the homogeneity of the diffusion boron-chromium layers.

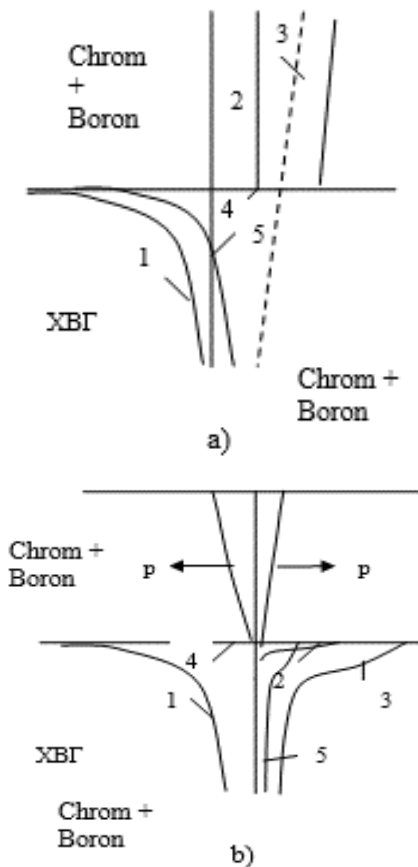


**Figure 1.** Schematic diagram of stress generation and redistribution in laser nanodiffusion complex boron-chromizing of paste-coated precision parts. (a) Mechanism of crack initiation and stress distribution on the surface before boron-chromizing. (b) Mechanism of crack formation and stress redistribution after the laser diffusion process. The upper region corresponds to the boron-chromium diffusion layer, the lower region to the XBF base steel. Curves: 1 - compressive stresses in diffusion-coated steels after mechanical processing; 2 - stresses in the steel after thermal processing; 3 - stresses arising during cyclic diffusion normalisation; 4 - temperature-induced stresses in the steel; 5 - resulting total stress in the surface layer.

The surface hardness of precision parts restored and strengthened by diffusion metallization is in the range of  $H_{100} = 18-21$  GPa. The microhardness of steel grades XBF and IIIX15 is slightly higher (18 and 17 GPa, respectively). The lowest hardness was achieved in steel P18 (16 GPa). This is explained by the fact that in addition to complex borides of iron, carbides and borides of tungsten, molybdenum and other alloying elements are also formed in the diffusion layer of this steel.

Regardless of the steel grades, the change in microhardness along the diffusion layer is not significant. A slight decrease in hardness is observed near the base of the layer, which is associated with a decrease in the amount of carbon, complex borides in this zone, and an increase in the share of solid solutions in iron [1].

After boron-chromizing plating, the initial hardness of

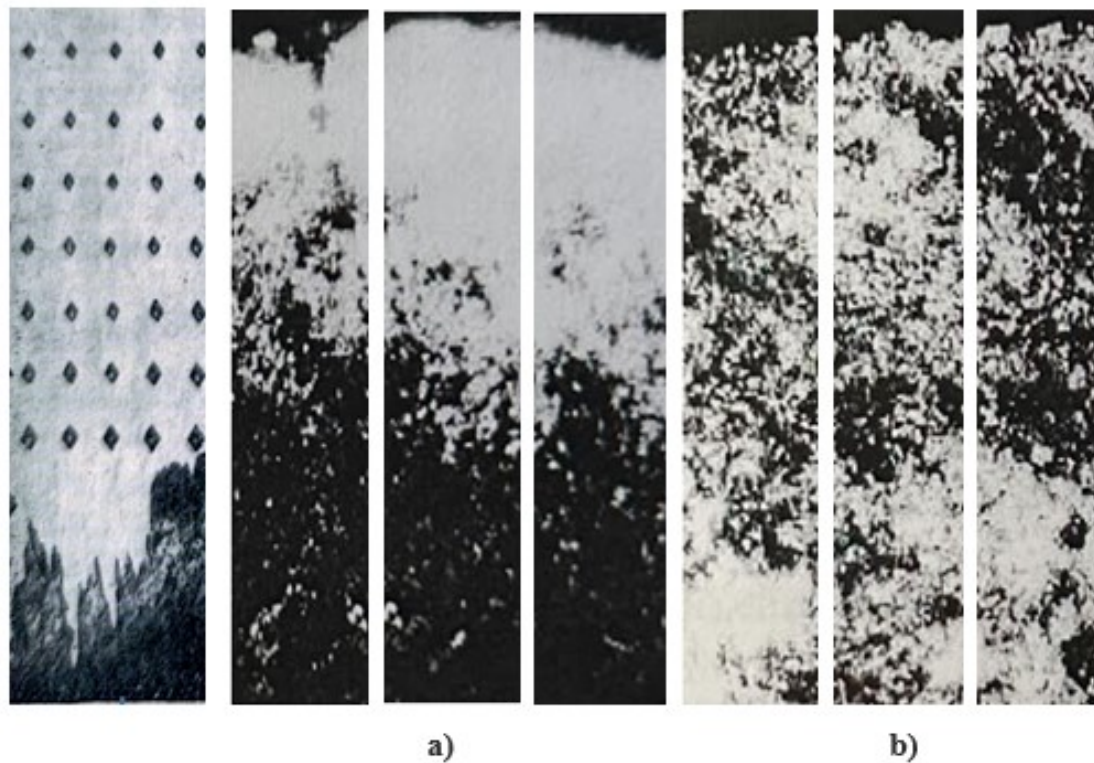


**Figure 2.** Microhardness and microstructure of diffusion boron-chromized layers on steels XBF and IIX15. Left: pattern of microhardness indents obtained with a PMT-3 microhardness tester along the cross-section of the diffusion layer. Centre and right: representative micrographs of the boron-chromium coating (a) and the underlying core (b) for steels XBF and IIX15 after diffusion boron-chromization ( $\times 450$ ).

the parts decreases significantly, which is explained by high-temperature annealing and recrystallization.

The microstructure of diffusion coatings was studied in the above-mentioned powder mixture after boron-chromizing for 4 hours at a temperature of 1000 °C. In boron-chromized steels, the diffusion layer does not have a needle-like structure, since the needles merge to form a solid coating. Under this coating, a fine network of borides is observed in XBF and IIX15 steels. The structure of the coating in Y8 and 30XГCA steels is similar to that in XBF and IIX15 steels, but a sublayer boride network is not formed here. In 18X2X4BA steel, the coating has a fine-grained structure. In 45 steel, a coating with less integrity was obtained. The diffusion layer is quite clearly visible and consists of needles of the same length. It should be noted that boride coatings do not form on nitrided parts made of 25X5MA steel. This is probably due to the active diffusion of nitrogen from the saturated surface. The diffusion boride coating is located on the steel surface in the form of an evenly distributed layer. The substrate is saturated with carbides of alloying elements and textured in the axial direction.

The results of x-ray structural phase analysis presented in Table 1 and Figure 2 show that during boron-chromizing, diffusion coatings consisting of complex borides of iron and chromizing are formed in the proposed powder mixture. Figure 2 combines the microhardness measurements with the corresponding microstructure of the diffusion boron-chromized layers on steels XBF and

IIX15. The left-hand image shows a regular array of PMT-3 microhardness indents made from the coating surface towards the substrate, which was used to construct the hardness profiles as a function of diffusion layer thickness. The micrographs labelled "a" correspond to the outer boron-chromium coating, where a dense, nearly continuous boride-rich layer is observed. The micrographs labelled "b" show the transition to the core of the steels, in which the diffusion layer gradually changes into the base microstructure of the XBF and IIX15 steels. The presence of a continuous boride-rich coating and a fine secondary boride network beneath it explains the high and relatively uniform microhardness values measured across the diffusion layer. Main phase in these coatings is low-boride  $(\text{Fe,Cr})_2\text{B}$ , which shows less brittleness. High-boride  $(\text{Fe,Cr})\text{B}$  is present only in small quantities on the surface of XBF and IIX15 steel samples and is no longer observed at a depth of 5 microns. In 45 steel, the amount of  $(\text{Fe,Cr})\text{B}$  boride on the surface is significantly higher. In XBF and IIX15 steels, the texturing of boride crystals begins already at a depth of 5 microns, and at a depth of 80 microns, a clear texture is observed in 45 steel. At a depth of 120–130 microns, the structure is a matrix of the base metal ( $\alpha\text{-Fe}$ ), reinforced with  $(\text{Fe,Cr})\text{B}$  boride needles. In steels XBF and IIX15, carbon displaced by boron is released in the form of  $\text{Fe}_3\text{C}$  carbides. In steel 45, boride crystals are arranged irregularly, which was confirmed by metallographic analysis. As a result, carbon diffusion occurs in the intercrystalline space, which is accompanied by the

**Table 1.** Results of x-ray structural phase analysis of coatings obtained after boron-chromization. T = 1100 °C, τ = 6 hours

Steel grade	Change of linear dimensions, μm	Layer thickness, μm	Surface roughness, Ra, μm	Microhardness, H <sub>μ</sub> GPa	Results of X-ray structural phase analysis by layers (distance from surface, μm):					
					Surface	10	50	100	120	150
XBΓ	256-264	346	1.2-1.6	21-21.2	(Fe,Cr) <sub>2</sub> B+ +(Fe,Cr)B*	(Fe,Cr) <sub>2</sub> B textured	(Fe,Cr) <sub>2</sub> B texture enhancement	(Fe,Cr) <sub>2</sub> B textured	(Fe,Cr) <sub>2</sub> B+ +αFe*	(Fe,Cr) <sub>2</sub> B+ +αFe+Fe <sub>3</sub> C*
IIIХ15	265-268	352-355	1.4-1.8	20-20.8	(Fe,Cr) <sub>2</sub> B+ +(Fe,Cr)B*	(Fe,Cr) <sub>2</sub> B textured	(Fe,Cr) <sub>2</sub> B texture enhancement	(Fe,Cr) <sub>2</sub> B texture enhancement	(Fe,Cr) <sub>2</sub> B+ +αFe*	(Fe,Cr) <sub>2</sub> B+ +αFe*
P18	120-124	170-175	1.2-1.6	20.6-20.8	-	-	-	-	-	-

\* The phases shown in the table are mainly composed of complex borides of iron and chromium, with lower borides acting as the dominant phases.

Abbreviations: XBΓ – chromium-tungsten-manganese alloyed steel used for fuel-pump precision parts; IIIХ15 – high-carbon chromium bearing steel; P18 – high-speed tool steel. Ra – arithmetic mean surface roughness; H<sub>μ</sub> – microhardness measured with a PMT-3 tester and expressed in MPa. α-Fe – ferritic matrix (α-iron); Fe<sub>3</sub>C – iron carbide (cementite).

The phases listed in the table are mainly complex borides of iron and chromium; low-boride phases such as (Fe,Cr)<sub>2</sub>B act as the dominant strengthening phase, while high-boride (Fe,Cr)B appears only in small amounts near the surface

formation of Fe<sub>3</sub>C carbides.

The study of the distribution of elements along the depth of the diffusion coatings showed that in XBΓ and IIIХ15 steels, there is no free carbon in the boride zone. In 45 steel, a zone of high carbon concentration is formed under the boride layer. Due to the irregular arrangement of boride crystals, diffusion occurs throughout the entire thickness of the coating, resulting in the formation of iron carbides. The chromium content in the diffusion layer of XBΓ and IIIХ15 steels increases to 4%, and in other steels to 2%. The change in the structure of the boride coating during boron-chromizing is most likely due to the formation of new phases based on Fe<sub>2</sub>B and FeB – (Fe,Cr)<sub>2</sub>B; (Fe,Cr)B; (Cr,Fe)<sub>2</sub>B; (Cr,Fe)B. At this time, the boride needles shorten, stop contacting each other, and this leads to a decrease in the brittleness of the coating.

The microhardness of the coatings obtained in experimental samples does not fall below the minimum limit set by the technical requirements of the manufacturer, which makes it possible to apply diffusion boron-chromizing for the restoration of precise machine and apparatus parts.

The hardness of coatings deposited by laser technology depends on the laser parameters (modes, power, deposition method, etc.) and is in some way related to the internal structure, residual stresses, porosity, etc. [14,15]. The microhardness of the surface layer of the samples is affected by the thickness of the coating layer at different laser modes. The modes of mechanical processing before diffusion metallization affect the microhardness of the complex boron-chrome coating. To clarify such cases, we studied the distribution of microhardness along the depth of polished chromium, titanium and complex boron-chrome coatings obtained at different temperatures (1150, 1100, 1050 and 1000 °C).

In comparison with other surface-hardening technologies reported in the literature, the microhardness values obtained in the present work are at the upper end of the range typically achieved for alloy steels. Laser surface hardening of crankshafts, ultra-high-strength alloys and other structural components usually results in surface microhardness levels of about 8–15 GPa, depending on composition and processing parameters [4–6]. Laser-

cladded and laser-deposited high-entropy alloy coatings show similarly high hardness, but often require relatively thick layers and complex multi-component chemistries to achieve such values [14,15]. In contrast, the vacuum nanodiffusion boron-chromium coatings investigated here reach 18–21 GPa while maintaining a diffusion-type bonding with the substrate, which makes them competitive with or superior to many conventional hardening and coating methods used for tribological applications.

These results are consistent with the general understanding that boride-rich diffusion layers and carbide-boride reinforced matrices provide excellent strengthening for components operating under severe contact loading [4–6]. At the same time, the present study extends previous work by linking the high microhardness and complex phase composition of the boron-chromium diffusion layer with the observed redistribution of residual stresses and the formation of a fine microcrack network. This combination of high hardness, diffusion bonding and controlled stress relaxation distinguishes vacuum laser diffusion boron-chromizing from more traditional nitriding, carburizing and hard-chromium plating processes, and explains its potential advantages for the restoration and strengthening of fuel pump precision parts.

### 3.1. Stress analysis and crack formation

The tribological performance of fuel pump precision parts is strongly controlled by the combination of surface hardness, phase composition, residual stresses and the presence of surface defects such as pores and microcracks. The results of the present study show that vacuum nanodiffusion boron-chromium coatings provide a relatively thick boride-rich diffusion layer with high microhardness (up to about 21 GPa), a stable hardness level within the diffusion zone and a fine secondary boride network in the subsurface region. Together with the predominantly compressive residual stress state and the presence of a controlled network of small microcracks, such a structure is expected to reduce the real contact area, stabilise the lubrication regime in the plunger-barrel pair and limit the propagation of critical cracks under cyclic loading.

From a tribological point of view, these features should

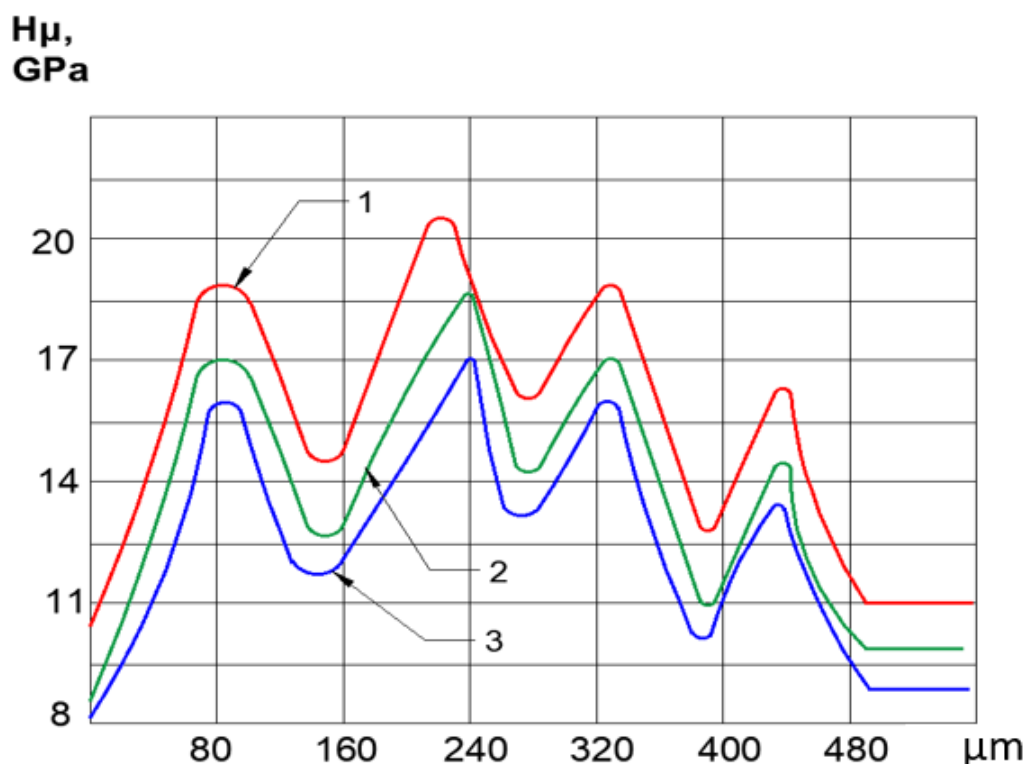


**Figure 3.** Variation of microhardness depending on the thickness of the diffusion layer formed by vacuum nanodiffusion metallization using laser-assisted paste deposition with a cyclic method.

lead to lower wear rates and more stable friction behaviour in comparison with untreated or conventionally hardened surfaces, in agreement with general trends reported for boride-based diffusion coatings and laser-hardened layers [4–6,14,15]. However, a quantitative assessment of the wear rate, friction coefficient evolution and damage mechanisms under service-like conditions requires dedicated tribological testing (for example, reciprocating or pin-on-disc tests) using lubricants and loads representative of high-pressure fuel pump operation. Such experiments are planned as a continuation of the present work in order to complement the microstructural and microhardness results with a full tribological characterisation of the diffusion boron–chromium coatings.

### 3.2. Hardness measurements

The microhardness of complex boron-chrome coatings was measured in five rows of inclined sections from the boundary of the base material to the surface of the coating. The distance between the cracks was 0.05 mm. The diffusion process was carried out at  $T = 1150\text{ }^{\circ}\text{C}$ ;  $\tau = 1$  second, and the cyclic duration was 5–6 minutes. The results of the microhardness of the diffusion complex boron-chrome coating are shown in figure 3. According to the measurements and the figure, it is clear that the microhardness is unevenly distributed. It was carried out on micrographs made of sample steels XBF, IIIX15 and P18 used in the manufacture of precision parts. Analysis of Fig. 3 shows that the maximum value of the hardness of steels XBF, IIIX15 and P18 is 21 GPa, 18.6 GPa and 17.6 GPa, respectively. The maximum hardness of XBF steel can

be achieved when the diffusion layer is 180  $\mu\text{m}$ , and in IIIX15 and P18 steels - when the diffusion layer is 240  $\mu\text{m}$  thick. The lowest hardness values were 11 GPa for XBF steel - 480  $\mu\text{m}$  thick, 10 GPa for IIIX15 steel - 380  $\mu\text{m}$  thick, and 8.8 GPa for P18 steel - 380  $\mu\text{m}$  thick.

Microhardness is distributed in the intervals only in deposits obtained at high temperatures. The microhardness of the boron-chrome coating applied at temperatures of 1000 and 1150 $^{\circ}\text{C}$  takes different values at different points. This distribution of microhardness along the cross section can be explained by the stratification of the deposit, i.e. it is formed as a result of the transition of layers of stable cubic crystal structure of chromium, titanium and boron-chromizing with layers consisting of unstable hexagonal crystal structure, completely or partially. Cracks can form every 10–15  $\mu\text{m}$  in non-diffusion coatings due to the influence of residual stresses when applying paste in vacuum with a laser.

The presence of cracks in the coating also affects the change in microhardness.

As the surface hardness increases, the wear resistance of the coating increases significantly.

The microhardness of the complex boron-chromium coating decreases by about 10% after one or two annealing processes for 2.5 h at 1200 $^{\circ}\text{C}$  and does not change with increasing number of annealings. The slight decrease in microhardness after heat treatment is a result of the formation of chromium and boron compound carbides in the surface layer, as well as the cracking of the coating and the reduction of residual stresses due to the different coefficients of volumetric expansion of the steel and the

coating. At the same time, the chemical composition and hardness of the steel affect the hardness of the chromium and complex boron-chromium coating without heat treatment or after heat treatment.

#### 4. Conclusion

1. The microhardness of laser surface-hardened and restored precision parts reaches about 21 GPa. After normalization heat treatment at 350–360 °C for 20–30 minutes the microhardness decreases by roughly 5–10 %, but remains in the range of 18–20 GPa and is practically independent of the base steel grade and its prior heat treatment.

2. Coatings obtained by vacuum nanodiffusion boron-chromium treatment with laser-assisted paste deposition exhibit high hardness and a significant diffusion depth into the base metal. Post-coating heat treatment (350–1000 °C for steel and copper-based alloys, 200–220 °C for aluminium alloys or high-frequency normalization for precision fuel-pump parts) increases the coating hardness up to  $(600\text{--}950) \cdot 10^7$  Pa while providing the required microstructure and phase composition, as confirmed by spectral analysis and X-ray diffraction.

3. For the investigated steels XBI, IIIX15 and P18, the diffusion boron-chromium layers maintain microhardness values above the minimum limits specified by the manufacturer and show only a moderate decrease in hardness with depth, which confirms the suitability of this technology for restoring and strengthening precision machine and apparatus parts.

4. Experimental results indicate that a fine network of small cracks formed during boron-chromizing of precision fuel-pump parts can play a predominantly positive role: these microcracks help to relieve residual stresses and regulate lubrication in the plunger-barrel contact, rather than acting as critical defects, thereby contributing to the operational reliability of the components.

#### References

- [1] A.G. Guseinov, Sh.N. Asadov. Life of parts restored by diffusional metallization. *Russian Engineering Research*, Volume 33, Issue 6, 2013, pp. 327–329. <https://doi.org/10.3103/S1068798X13060075>
- [2] A. Huseynov, F. Huseynli, M. Safarov. Reliability prediction of precision parts of fuel pumps with enhanced surface hardness achieved through laser technology. *Tribologia – Finnish Journal of Tribology*, 42(1–2), 2025, pp. 64–71. <https://doi.org/10.30678/fjt.152491>
- [3] A. Huseynov, I. Nazarov, F. Huseynli, M. Safarov. Determination of deformation and machining allowance of precision parts hardened by laser method. *Reliability: Theory & Applications, Special Issue No. 7 (83), Volume 20, 2025*, pp. 379–385. <https://doi.org/10.24412/1932-2321-2025-783-379-385>
- [4] Huizhi Peng, Shun Wu, Wen Hao Kan, Samuel Chao Voon Lim, Yuman Zhu, Aijun Huang. Rapid hardening response of ultra-hard Ti-6Al-2Sn-4Zr-6Mo alloy produced by laser powder bed fusion. *Scripta Materialia*, Volume 226, 2023, Article 115209. <https://doi.org/10.1016/j.scriptamat.2022.115209>
- [5] Zhenyu Chen, Xiaodong Yu, Ning Ding, Jianchen Cong, Jun Sun, Qingbo Jia, Chuanyang Wang. Wear resistance enhancement of QT700-2 ductile iron crankshaft processed by laser hardening. *Optics & Laser Technology*, Volume 164, 2023, Article 109519. <https://doi.org/10.1016/j.optlastec.2023.109519>
- [6] Senthil Kumar P., Jegadheesan C., Somasundaram P., Praveen Kumar S., Vivek Anand A., Ajit Pal Singh, Jeyaprakash N. State of art: review on laser surface hardening of alloy metals. *Materials Today: Proceedings*, 2023. <https://doi.org/10.1016/j.matpr.2023.04.259>
- [7] Kui Zhan, Yijin Luo, Ying Zeng. Application of short-pulsed CO<sub>2</sub> laser and long-pulsed Nd:YAG laser in the treatment of severe hypertrophic port-wine stains. *Chinese Journal of Plastic and Reconstructive Surgery*, Volume 4, Issue 3, 2022, pp. 140–143. <https://doi.org/10.1016/j.cjpr.2022.08.006>
- [8] A. Huseynov, A. Holding, F. Huseynli, M. Safarov. Challenges of property inheritance during the technological processing of fuel pump precision parts. *Tribologia – Finnish Journal of Tribology*, 42(1–2), 2025, pp. 72–79. <https://doi.org/10.30678/fjt.160975>
- [9] Qionghuan Zeng, Yiming Chen, Zhongsheng Yang, Lei Zhang, Zhijun Wang, Lei Wang, Junjie Li, Jincheng Wang. Effect of grain size and grain boundary type on intergranular stress corrosion cracking of austenitic stainless steel: a phase-field study. *Corrosion Science*, Volume 241, 2024, Article 112557. <https://doi.org/10.1016/j.corsci.2024.112557>
- [10] M. Ciavarella. A graded elastic modulus concept to eliminate stress or strain energy density singularity at sharp notches and cracks, with consequent elimination of size-scale effect on strength. *European Journal of Mechanics – A/Solids*, Volume 109, 2025, Article 105477. <https://doi.org/10.1016/j.euromechsol.2024.105477>
- [11] Qiang Lin, Bin Yang, Lin Liu, Xinyu Yao, Haohao Ding, Shuyue Zhang, Min Yang, Qian Xiao, Wenjian Wang. Acoustic emission signal characteristics of crack and porosity defects formation during laser cladding WC/Fe313 coatings. *NDT & E International*, Volume 155, 2025, Article 103404. <https://doi.org/10.1016/j.ndteint.2025.103404>
- [12] Jianjun Xie, Huanjie Fang, Yongxin Wang, Wenqian Wang, Jianhao Yu, Jicheng Li, Xiaodong He, Jibin Pu. Controlling the porosity to enhance the high-

temperature tribological performance of plasma-sprayed NiCr-Cr<sub>3</sub>C<sub>2</sub>-BaF<sub>2</sub>/CaF<sub>2</sub> coating by adopting axial feeding. *Journal of Materials Research and Technology*, Volume 36, 2025, pp. 2577-2588. <https://doi.org/10.1016/j.jmrt.2025.03.273>

- [13] M.F.C. Ordoñez, D.L. Rodrigues, A.P. Tschiptschin, R.M. Souza. Effect of porosity on surface deformation and subsurface layer produced by scratch tests of sintered low-alloy steel. *Tribology International*, Volume 209, 2025, Article 110674. <https://doi.org/10.1016/j.triboint.2025.110674>
- [14] Yahong Xu, Dazhong Wang, Shujing Wu, Haoxiang Lu, Rao Yao, Jin Yang, Feng Jiang, Takao Akiyama. Research progress on defect formation mechanism and process optimization of laser cladding high entropy alloy coatings. *Optics & Laser Technology*, Volume 187, 2025, Article 112819. <https://doi.org/10.1016/j.optlastec.2025.112819>
- [15] Zia Ullah Arif, Muhammad Yasir Khalid, Ans Al Rashid, Ehtsham ur Rehman, Muhammad Atif. Laser deposition of high-entropy alloys: a comprehensive review. *Optics & Laser Technology*, Volume 145, 2022, Article 107447. <https://doi.org/10.1016/j.optlastec.2021.107447>